

A $j_{\text{eff}} = 1/2$ Pseudospin Continuum in CaIrO_3

Matteo Rossi,^{1,2,*} Pietro Marabotti,² Yasuyuki Hirata,^{3,†} Giulio Monaco,⁴ Michael Krisch,¹ Kenya Ohgushi,^{3,‡} Krzysztof Wohlfeld,⁵ Jeroen van den Brink,^{6,7} and Marco Moretti Sala^{1,2,§}

¹ESRF – The European Synchrotron, 71 Avenue des Martyrs, CS 40220, F-38043 Grenoble, France

²Dipartimento di Fisica, Politecnico di Milano, Piazza Leonardo da Vinci 32, I-20133 Milano, Italy

³Institute for Solid State Physics, The University of Tokyo, Kashiwa, Chiba 277-8581, Japan

⁴Dipartimento di Fisica, Università di Trento, via Sommarive 14, I-38123 Povo (TN), Italy

⁵Institute of Theoretical Physics, Faculty of Physics, University of Warsaw, Pasteura 5, PL-02093 Warsaw, Poland

⁶Institute for Theoretical Solid State Physics, IFW Dresden, Helmholtzstrasse 20, D-01069 Dresden, Germany

⁷Department of Physics, Technical University Dresden, D-01062 Dresden, Germany

In so-called $j_{\text{eff}} = 1/2$ systems, including some iridates and ruthenates, the coherent superposition of t_{2g} orbitals in the ground state gives rise to hopping processes that strongly depend on the bond geometry. Resonant inelastic x-ray scattering (RIXS) measurements on CaIrO_3 reveal a prototypical $j_{\text{eff}} = 1/2$ pseudospin continuum, a hallmark of one-dimensional (1D) magnetic systems despite its three-dimensional crystal structure. The experimental spectra compare very well to the calculated magnetic dynamical structure factor of weakly coupled spin-1/2 chains. We attribute the onset of such quasi-1D magnetism to the fundamental difference in the magnetic interactions between the $j_{\text{eff}} = 1/2$ pseudospins along the corner- and edge-sharing bonds in CaIrO_3 .

I. INTRODUCTION

Spin-orbit-induced Mott insulators, including iridium oxides (iridates) and RuCl_3 , host a large variety of physical properties, whose microscopic origin is intrinsic to the nature of the $j_{\text{eff}} = 1/2$ ground state and of the interactions it gives rise to [1–4]. Electronic interactions in insulating systems originate from virtual hopping processes, possibly through the ligands and, depending on the bond geometry, multiple hopping paths may exist. This possibility is enhanced in iridates, where the $j_{\text{eff}} = 1/2$ electronic wave function arises from a coherent superposition of all t_{2g} orbitals with mixed phases and spin components. As a consequence, magnetic interactions in corner-, edge-, or face-sharing octahedral iridates are drastically different [5–9].

Corner-sharing layered-perovskite iridates bear isotropic Heisenberg-like antiferromagnetic (AFM) exchange interactions between $j_{\text{eff}} = 1/2$ pseudospins, with a small symmetric anisotropic contribution [5]. Indeed, materials featuring corner-sharing IrO_6 octahedra on a quasi-two-dimensional (2D) square lattice, including Sr_2IrO_4 [2, 10–12], $\text{Sr}_3\text{Ir}_2\text{O}_7$ [13–16] and Ba_2IrO_4 [17, 18], display magnetic properties reminiscent of cuprates [19–27] and attracted the interest of the scientific community – even more so when unconventional

superconductivity was predicted in such iridates [28–31]. Distortions of the ideal bond geometry affect both the nature and strength of the exchange interactions. For example, if the corner-sharing bond lacks inversion symmetry, an antisymmetric exchange anisotropy is allowed; Dzyaloshinski-Moriya interaction sets in and induces a finite canting of the magnetic moments away from the perfectly collinear structure, thus giving rise to weak ferromagnetism in Sr_2IrO_4 [2, 12].

For edge-sharing IrO_6 octahedra, instead, the hopping paths via the two bridging oxygens interfere in a destructive manner and can cause the cancellation of the isotropic exchange interaction [5]. As a result, a weak Ising-like anisotropic interaction dominates, which gives rise to Kitaev-like spin-spin exchange [9, 32, 33]. Particularly interesting are materials composed of edge-sharing IrO_6 octahedra on a honeycomb (Na_2IrO_3 [32, 34–36], $\alpha\text{-Li}_2\text{IrO}_3$ [35]), hyper- ($\beta\text{-Li}_2\text{IrO}_3$ [37]) and stripy- ($\gamma\text{-Li}_2\text{IrO}_3$ [38]) honeycomb structure as they sustain Kitaev frustration and are therefore candidates for unconventional quantum ground states and excitations such as spin liquid ground states that can harbour Majorana fermions [9, 33, 39]. However, the Kitaev interaction is usually not very strong and other magnetic couplings, otherwise irrelevant, can induce long-range magnetically-ordered phases [40–44]. Face-sharing iridates, on the other hand, are not yet fully explored, but allow for intriguing properties. For example, iridates featuring Ir_2O_9 bioctahedra on a triangular lattice, including $\text{Ba}_3(\text{Ti,Zr,Ce,Pr,Tb})\text{Ir}_2\text{O}_9$ [45, 46], show excessively small values of the effective magnetic moments possibly due to covalency effects [7, 8, 47].

The various types of interactions on the bond geometries described above are characterized by very distinct energy scales: the Kitaev interaction in edge-sharing systems is about an order of magnitude smaller

* rossim@stanford.edu; Present address: Stanford Institute for Materials and Energy Sciences, SLAC National Accelerator Laboratory, 2575 Sand Hill Road, Menlo Park, CA 94025, USA.

† Present address: Department of Applied Physics, National Defense Academy of Japan, 1-10-20 Hashirimizu, Yokosuka, Kanagawa 2398686, Japan.

‡ Present address: Department of Physics, Tohoku University, 6-3 Aramaki-Aoba, Aoba-ku, Sendai, Miyagi 980-8578, Japan.

§ marco.moretti@polimi.it

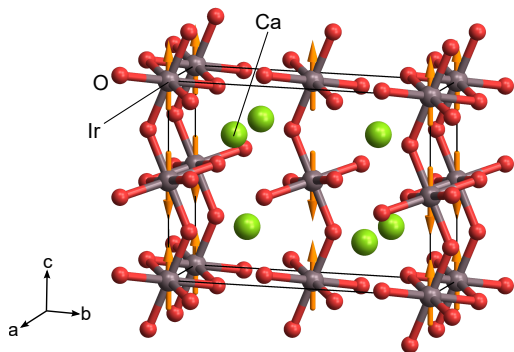


FIG. 1. Crystal and magnetic structure of CaIrO_3 . Ir ions (grey spheres) are surrounded by octahedra of O ions (red spheres) sharing an edge and a corner along the a and c axes, respectively. Layers of Ca ions (green spheres) separate the ac planes. $j_{\text{eff}} = 1/2$ pseudospins are displayed as orange arrows.

than the Heisenberg exchange in corner-sharing systems. However, material-dependent properties could also affect the origin and magnitude of the superexchange, as discussed above. Thus, we here consider the post-perovskite CaIrO_3 , whose crystal structure features both edge-sharing IrO_6 octahedra along the a axis and corner-sharing octahedra along the orthogonal c direction (see Fig. 1). Even if the crystal structure is quasi 2D, with IrO planes separated by Ca spacers, we find evidence of quasi 1D magnetic dynamics. By means of resonant inelastic x-ray scattering (RIXS), we observe the dispersion of pseudospinons in a $j_{\text{eff}} = 1/2$ spin-orbit Mott insulator for the first time. The reduced dimensionality is strictly related to the nature of the $j_{\text{eff}} = 1/2$ ground state on the bond geometries and not guaranteed by crystallography alone. Our results are in agreement with the proposed striped AFM order [48] and theoretical predictions by *ab initio* quantum chemical calculations [49]. Our findings provide a new direction to tailor the magnetic properties of $j_{\text{eff}} = 1/2$ systems while pertaining a higher-dimensional lattice.

II. EXPERIMENTAL DETAILS

Single crystals of CaIrO_3 were grown using the flux method described in Ref. 48. Crystals have a needle shape with length of ~ 1 mm and diameter of ~ 0.1 mm. CaIrO_3 grows in the post-perovskite crystal structure (space group $Cmcm$), with lattice parameters $a = 3.147$ Å, $b = 9.863$ Å and $c = 7.299$ Å [50, 51]. IrO_6 octahedra share an edge along the a direction and a corner along the c direction (Fig. 1). Below the Néel temperature $T_N \approx 110$ K [50–53], $j_{\text{eff}} = 1/2$ pseudospins order in a striped magnetic structure: magnetic moments are mostly aligned parallel to the c axis and are ferromagnetically (antiferromagnetically) coupled along the a (c) direction [48], as shown in Fig. 1.

Iridium L_3 edge (~ 11.22 keV) RIXS measurements were performed at the inelastic X-ray scattering beamline ID20 of ESRF – The European Synchrotron (Grenoble, France) [54, 55]. The incident beam was monochromated using a Si(844) back-scattering channel-cut crystal. The spectrometer is based on the Rowland circle geometry and is equipped with a single $R = 1$ m Si(844) diced crystal analyzer and a two-dimensional Maxipix detector [56]. A mask with circular aperture of 30 mm was installed in front of the analyzer to improve the momentum resolution. The overall energy and momentum resolutions were 35 meV (full width at half maximum) and approximately 0.2 Å $^{-1}$, respectively. The sample was cooled by means of a cryostat using He as exchange gas [57].

III. RESULTS AND DISCUSSION

The RIXS response of CaIrO_3 has been discussed by Moretti Sala *et al.* [58], who investigated the excitations at energy losses above 0.4 eV and ascribed those to electronic transitions within the t_{2g} manifold. In agreement with quantum chemical calculations [49, 59, 60], the analysis of RIXS data based on a single-ion model [1, 61, 62] shows that the ground state of CaIrO_3 departs from the ideal $j_{\text{eff}} = 1/2$ wave function, with the single hole unequally distributed among the t_{2g} orbitals [58]. In particular, it was found that the hole has predominant ($|d_{yz}, \pm\rangle \mp i|d_{xz}, \pm\rangle$)/ $\sqrt{2}$ character [58]. A priori, this might have implications on the bond-geometry dependence of the magnetic interactions; however, we note that the exchange processes in CaIrO_3 mostly involve the Ir d_{yz} and d_{xz} orbitals in both bond geometries and, since the phase and relative occupancies of these states are preserved, the nature of the dominant exchange interactions should be unaffected. We note that the hopping involving the e_g states can be safely neglected due to the large cubic crystal field (typically ~ 3 eV in iridates [63]).

We here focus on the spectral features at energy losses below 0.4 eV and on their momentum dependence. RIXS measurements along high-symmetry directions in reciprocal space were taken at 40 K and are shown in Fig. 2(a), (b) and (c). We first note that an excitation continuum extending up to ~ 0.3 eV appears in all high-symmetry directions and that it looks “gapped” everywhere in reciprocal space. The continuum behaves very differently in the three orthogonal directions. Specifically, along the H (edge-sharing) [Fig. 2(a)] and K [Fig. 2(b)] directions, the energy of the main peak is minimum and shows little and no momentum dependence, respectively. On the opposite, along the L (corner-sharing) direction [Fig. 2(c)], the RIXS spectra show a pronounced momentum dependence and the dispersion of the continuum is characterized by a double-arched shape: the low-energy boundary has a periodicity of 1 r.l.u., while the high energy envelope has double periodicity. We note immediately that the magnetic excitations of CaIrO_3 are markedly distinct from the ones of other layered iridates such as

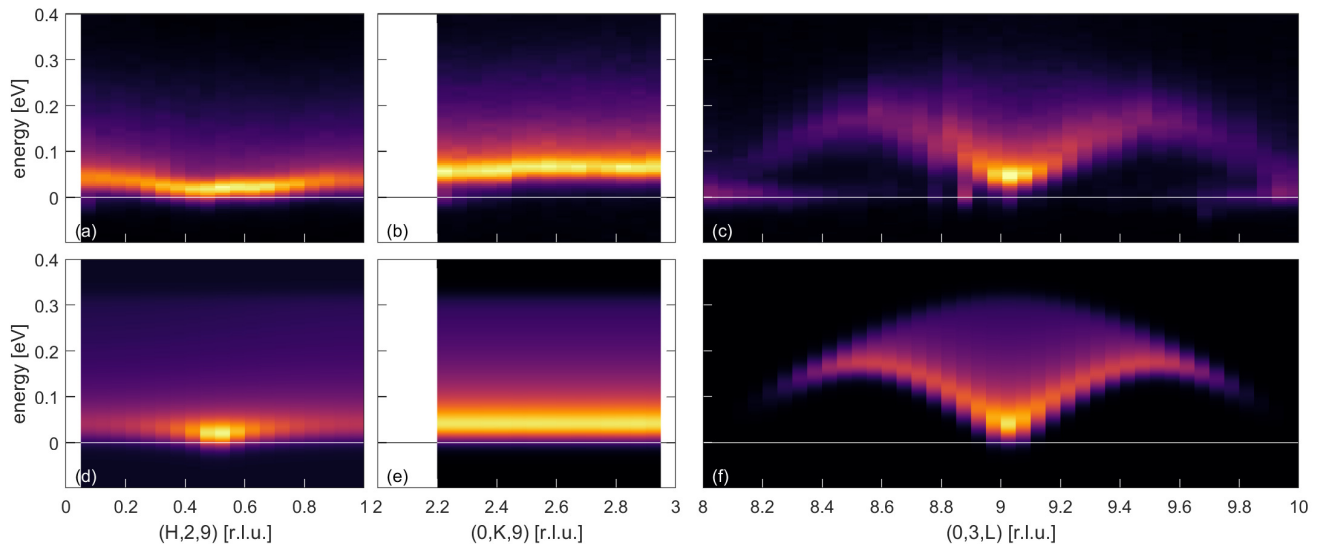


FIG. 2. RIXS intensity maps of CaIrO_3 measured at 40 K as a function of momentum transfer along the H (a), K (b), and L (c) high-symmetry directions of the reciprocal lattice. Panels (d), (e) and (f) display the magnetic dynamical structure factor of weakly coupled $S = 1/2$ chains computed for $J_c = 98$ meV and $J_a = -4.4$ meV.

Sr_2IrO_4 [19], $\text{Sr}_3\text{Ir}_2\text{O}_7$ [14, 64] and Na_2IrO_3 [32]. Instead, the momentum dependence of RIXS spectra observed in Fig. 2(c) is reminiscent of the dynamics of 1D AFM $S = 1/2$ chains [65–75]. In these systems, magnetic excitations are quasiparticles called spinons [65]: in a simple picture, spinons are domain walls that separate two degenerate regions of 1D AFM chains with out-of-phase spin order; they are created in pairs when a spin is excited within the chain. Since the two spinons can freely propagate along the chain with no energy cost, the $S = 1$ excitation dissociates into two independent entities carrying $S = 1/2$ each. This process, called fractionalization, is a hallmark of 1D AFM $S = 1/2$ chains. In the non-interacting picture, a two-spinon excitation can be considered as the excitation of two, independent single spinons, giving rise to the peculiar energy-momentum continuum [65]. Based on the similarity between the two-spinon continuum and the excitation spectrum of CaIrO_3 , we assign the latter to magnetic excitations of 1D AFM chains. In the case of CaIrO_3 , precautions should be taken because the magnetic moments are not $S = 1/2$ spins, but pseudospins that carry orbital angular momentum apart from the spin one. However, Fig. 2(c) is an unmistakable signature of the quasi-1D nature of the magnetic excitations of CaIrO_3 and, as shown below, provides the first experimental evidence of fractionalization of *pseudospinons* in a spin-orbit Mott insulator. CaIrO_3 is also one of the very few compounds exhibiting fractionalization that are not based on $3d$ transition metals.

In order to verify the above hypothesis and quantify the strength of the magnetic couplings in CaIrO_3 , we compare our RIXS results to the calculated magnetic dynamical structure factor $S(\mathbf{Q}, \omega)$. We first consider the magnetic dynamical structure factor $S_{1\text{D}}(q_z, \omega)$ of a 1D

AFM $S = 1/2$ chain with isotropic magnetic coupling $J_c > 0$, where $q_z = 2\pi L/c$ is the momentum transfer along the chain direction: it was derived by Müller *et al.* [76] and is characterized by a gapless double-arched excitation continuum, without momentum dependence perpendicular to the chain. However, the weak dispersion along the H direction shown in Fig. 2(a) suggests that a minimal model aiming at describing CaIrO_3 should include a magnetic coupling perpendicular to the chain direction J_a , which we assume to be isotropic for simplicity and negative to account for the FM alignment of the magnetic moments along the a direction [48]. Within the random phase approximation [77], the relation between the magnetic susceptibility of weakly coupled chains $\chi(\mathbf{Q}, \omega)$ and that of a 1D $S = 1/2$ chain $\chi_{1\text{D}}(q_z, \omega)$ is [77–79]:

$$\chi(\mathbf{Q}, \omega) = \frac{\chi_{1\text{D}}(q_z, \omega)}{1 - 2J_a \cos(q_x) \chi_{1\text{D}}(q_z, \omega)}, \quad (1)$$

where $q_x = 2\pi H/a$ is the momentum transfer perpendicular to the chain direction. The magnetic dynamical structure factor is related to the imaginary part of the magnetic susceptibility: $S(\mathbf{Q}, \omega) = -\chi''(\mathbf{Q}, \omega)$. A similar relationship holds for $S_{1\text{D}}(q_z, \omega)$ and $\chi''_{1\text{D}}(q_z, \omega)$. This approach has been extensively used to simulate the magnetic dynamical structure factor of systems characterized by weakly coupled magnetic chains as measured by inelastic neutron scattering [80–82].

Before any comparison to the experimental results is made, the calculated $S(\mathbf{Q}, \omega)$ should be broadened by the finite energy and momentum resolutions. The latter is determined by the analyzer surface and depends on the scattering geometry, as detailed in Ref. 55. The effect of a finite momentum resolution is critical near the Brillouin zone center ($q_z = 0$) and close to the zone boundaries

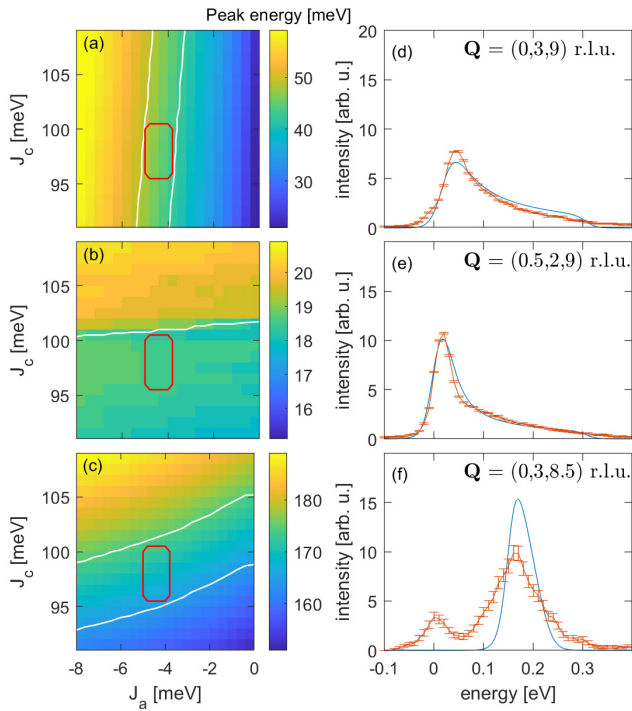


FIG. 3. Calculations of the magnetic peak position from $S(\mathbf{Q}, \omega)$ as a function of J_a and J_c for (a) $\mathbf{Q} = (0, 3, 9)$ r.l.u., (b) $\mathbf{Q} = (0.5, 2, 9)$ r.l.u. and (c) $\mathbf{Q} = (0, 3, 8.5)$ r.l.u.. The experimental peak position falls within the domains represented by white lines. The intersection of these three domains is enclosed by red circles. (d), (e) and (f) show the comparison between RIXS spectra (red) and $S(\mathbf{Q}, \omega)$ (blue solid lines) calculated for the optimal values $J_c = 98$ meV and $J_a = -4.4$ meV.

($q_z = \pm\pi$), where the dispersion of magnetic excitations is the steepest: indeed, it seems to artificially open a gap in the magnetic excitations spectrum, which, for a system of $S = 1/2$ spins interacting through isotropic couplings only, is gapless [66, 69].

In Fig. 3(a), (b) and (c), we extracted the energies of the magnetic peak from the calculated $S(\mathbf{Q}, \omega)$ as a function of J_a and J_c for three representative transferred momenta; white contour lines correspond to the magnetic peak position as determined by RIXS, *i.e.* 45 ± 3 meV at $\mathbf{Q} = (0, 3, 9)$ r.l.u., 18 ± 1 meV at $\mathbf{Q} = (0.5, 2, 9)$ r.l.u. and 170 ± 5 meV at $\mathbf{Q} = (0, 3, 8.5)$ r.l.u.. The intersection of these domains is a very small region of the $\{J_a, J_c\}$ parameter space enclosed by the red solid line. In particular, the best fit to the data is obtained for $J_a = -4.4$ meV and $J_c = 98$ meV. The magnitudes of the magnetic couplings beautifully confirm the predictions of quantum chemical calculations [49]. The magnetic dynamical structure factors capture the corresponding RIXS spectra, as shown in Fig. 3(d), (e) and (f). We note that the magnetic excitations measured at $\mathbf{Q} = (0, 3, 8.5)$ r.l.u. are broader than the corresponding dynamical structure factor (Fig. 3(f)). This is surprising given the excellent agreement at other momenta and

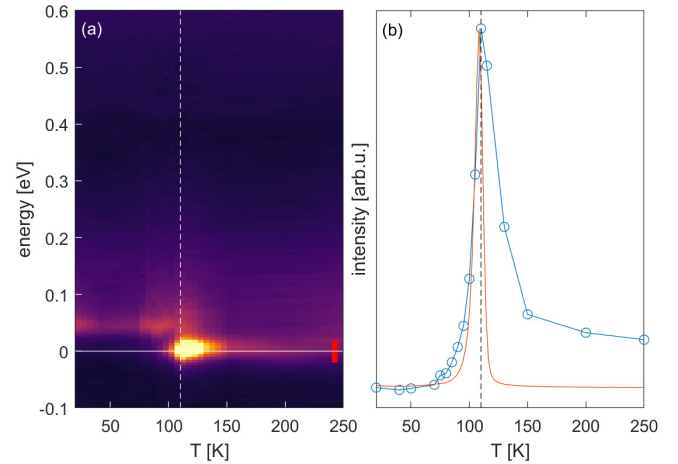


FIG. 4. (a) RIXS intensity map as a function of temperature at $\mathbf{Q} = (1, 2, 9)$ r.l.u. showing the strong maximum of the quasielastic signal at the Néel temperature (dashed line). (b) Temperature dependence of the quasielastic region of the RIXS spectra (blue open circles) obtained by integrating the RIXS signal in the energy window of ± 20 meV, represented by the red vertical bar in panel (a). The red solid line is the imaginary part of the quasi-static magnetic susceptibility, reported from Refs. 52 and 53.

will be the subject of further investigation. The full momentum dependence of the calculated $S(\mathbf{Q}, \omega)$ along the orthogonal H , K and L directions in reciprocal space is compared to the RIXS spectra in Fig. 2: the magnetic dynamical structure factor of weakly coupled ($|J_a| \ll J_c$) 1D AFM $S = 1/2$ chains satisfactorily reproduces the main features observed in our experimental results.

Before concluding, we report in Figure 4(a) the temperature dependence of RIXS spectra at momentum transfer $\mathbf{Q} = (1, 2, 9)$ r.l.u.. The two-spinon continuum is present at all temperatures. At high temperature, the spectra are characterized by a barely visible elastic line. When the sample is cooled down, the elastic peak intensity increases with a maximum at the magnetic phase transition and then decreases to complete suppression below 70 K. The trend of the elastic line is captured by the blue circles plotted in Fig. 4(b), which reports the temperature dependence of the RIXS signal integrated over an energy window of ± 20 meV centered around zero energy loss, highlighted as a red rectangle in Fig. 4(a). Its resemblance with the temperature dependence of the imaginary part of the quasi-static magnetic susceptibility (red solid line) [52, 53] suggests that also the elastic peak contains contributions from magnetic fluctuations. These are characterized by very small magnetic couplings and their temperature evolution catches the transition from the paramagnetic to the (3D) long-range AFM ordered phase, although $\mathbf{Q} = (1, 2, 9)$ r.l.u. does not correspond to a magnetic Bragg peak.

For the sake of completeness, we address two main limitations of our approach: i) higher-order spinon ex-

citations may give a minor contribution to the magnetic signal [69], but are neglected in our calculations for simplicity because the core-hole lifetime at the Ir L_3 edge is very small; ii) in the calculation of the magnetic dynamical structure factor, we considered two isotropic magnetic couplings only. However, the C_{2h} and C_{2v} point group symmetry of the edge- and corner-sharing bonds allows for symmetric [5, 6] and antisymmetric (Dzyaloshinski-Moriya) [83] anisotropic interactions along the a and c directions, respectively. The latter is responsible for the canting of the magnetic moments observed in CaIrO_3 [48], while the former possibly includes the Kitaev interaction. Unfortunately, a precise determination of all exchange parameters of CaIrO_3 , especially very small ones, is not possible at the present stage. However, one can say that the anisotropic Kitaev interaction across the edge-sharing direction is much smaller than the Heisenberg interaction along the corner-sharing bond, which is consistent with Jackeli and Khaliullin’s argument [5].

IV. CONCLUSIONS

To summarize, we investigated the magnetic dynamics of CaIrO_3 by means of RIXS and found strong evidence for quasi-1D magnetic behavior. Specifically, we interpreted the momentum dependence of the magnetic dynamics as due to $j_{\text{eff}} = 1/2$ pseudospin excitations. Theoretical calculations of the magnetic dynamical structure factor of weakly coupled AFM chains adequately re-

produce the experimental observations. Our results provide the first evidence of a pseudospin continuum in spin-orbit Mott insulators. Our findings are consistent with the prediction of a strong bond-dependence of the magnetic couplings in iridates [5, 6], which lowers the effective dimensionality of magnetism in CaIrO_3 and provides a strategy to engineer the magnetic properties of $j_{\text{eff}} = 1/2$ materials within their higher-dimensional lattice.

ACKNOWLEDGMENTS

M. Rossi and M. Moretti Sala kindly acknowledge C. Henriquet and R. Verbeni for technical assistance during the experiment and D. K. Singh for providing the magnetic susceptibility data of CaIrO_3 . M. Rossi would like to thank S. Toth for helpful discussions. K. Wohlfeld acknowledges support of the National Science Center (NCN), Project No. 2016/22/E/ST3/00560. J.v.d.B acknowledges financial support from the German Research Foundation (Deutsche Forschungsgemeinschaft, DFG) via SFB1143 project A5 and supported by the DFG through the Würzburg-Dresden Cluster of Excellence on Complexity and Topology in Quantum Matter - ct.qmat (EXC 2147, project id 39085490).

This is a pre-print of an article published in The European Physical Journal Plus. The final authenticated version is available online at: <https://doi.org/10.1140/epjp/s13360-020-00649-5>.

-
- [1] B. J. Kim, Hosub Jin, S. J. Moon, J.-Y. Kim, B.-G. Park, C. S. Leem, Jaejun Yu, T. W. Noh, C. Kim, S.-J. Oh, J.-H. Park, V. Durairaj, G. Cao, and E. Rotenberg, “Novel $J_{\text{eff}} = 1/2$ Mott State Induced by Relativistic Spin-Orbit Coupling in Sr_2IrO_4 ,” *Phys. Rev. Lett.* **101**, 076402 (2008).
 - [2] B. J. Kim, H. Ohsumi, T. Komesu, S. Sakai, T. Morita, H. Takagi, and T. Arima, “Phase-Sensitive Observation of a Spin-Orbital Mott State in Sr_2IrO_4 ,” *Science* **323**, 1329–1332 (2009).
 - [3] William Witczak-Krempa, Gang Chen, Yong Baek Kim, and Leon Balents, “Correlated Quantum Phenomena in the Strong Spin-Orbit Regime,” *Annu. Rev. Condens. Matter Phys.* **5**, 57–82 (2014).
 - [4] Jeffrey G. Rau, Eric Kin-Ho Lee, and Hae-Young Kee, “Spin-Orbit Physics Giving Rise to Novel Phases in Correlated Systems: Iridates and Related Materials,” *Annu. Rev. Condens. Matter Phys.* **7**, 195–221 (2016).
 - [5] G. Jackeli and G. Khaliullin, “Mott Insulators in the Strong Spin-Orbit Coupling Limit: From Heisenberg to a Quantum Compass and Kitaev Models,” *Phys. Rev. Lett.* **102**, 017205 (2009).
 - [6] H. Matsuura and M. Ogata, “A Poor Mans Derivation of Quantum Compass Heisenberg Interaction: Superexchange Interaction in JJ Coupling Scheme,” *J. Phys. Soc. Jpn.* **83**, 093701 (2014).
 - [7] K. I. Kugel, D. I. Khomskii, A. O. Sboychakov, and S. V. Streltsov, “Spin-orbital interaction for face-sharing octahedra: Realization of a highly symmetric $\text{SU}(4)$ model,” *Phys. Rev. B* **91**, 155125 (2015).
 - [8] D. I. Khomskii, K. I. Kugel, A. O. Sboychakov, and S. V. Streltsov, “Role of local geometry in the spin and orbital structure of transition metal compounds,” *J. Exp. Theor. Phys.* **122**, 484–498 (2016).
 - [9] Hidenori Takagi, Tomohiro Takayama, George Jackeli, Giniyat Khaliullin, and Stephen E. Nagler, “Concept and realization of Kitaev quantum spin liquids,” *Nat. Rev. Phys.* **1**, 264–280 (2019).
 - [10] M. K. Crawford, M. A. Subramanian, R. L. Harlow, J. A. Fernandez-Baca, Z. R. Wang, and D. C. Johnston, “Structural and magnetic studies of Sr_2IrO_4 ,” *Phys. Rev. B* **49**, 9198–9201 (1994).
 - [11] G. Cao, J. Bolivar, S. McCall, J. E. Crow, and R. P. Guertin, “Weak ferromagnetism, metal-to-nonmetal transition, and negative differential resistivity in single-crystal Sr_2IrO_4 ,” *Phys. Rev. B* **57**, R11039–R11042 (1998).
 - [12] S. Boseggia, H. C. Walker, J. Vale, R. Springell, Z. Feng, R. S. Perry, M. Moretti Sala, H. M. Rønnow, S. P. Collins, and D. F. McMorrow, “Locking of iridium magnetic moments to the correlated rotation of oxygen octahedra in Sr_2IrO_4 revealed by x-ray resonant scattering,” *J. Phys. Condens. Matter* **25**, 422202 (2013).

- [13] G. Cao, Y. Xin, C. S. Alexander, J. E. Crow, P. Schlottmann, M. K. Crawford, R. L. Harlow, and W. Marshall, "Anomalous magnetic and transport behavior in the magnetic insulator $\text{Sr}_3\text{Ir}_2\text{O}_7$," *Phys. Rev. B* **66**, 214412 (2002).
- [14] Jung-ho Kim, A. H. Said, D. Casa, M. H. Upton, T. Gog, M. Daghofer, G. Jackeli, J. van den Brink, G. Khaliullin, and B. J. Kim, "Large Spin-Wave Energy Gap in the Bilayer Iridate $\text{Sr}_3\text{Ir}_2\text{O}_7$: Evidence for Enhanced Dipolar Interactions Near the Mott Metal-Insulator Transition," *Phys. Rev. Lett.* **109**, 157402 (2012).
- [15] S. Boseggia, R. Springell, H. C. Walker, A. T. Boothroyd, D. Prabhakaran, S. P. Collins, and D. F. McMorrow, "On the magnetic structure of $\text{Sr}_3\text{Ir}_2\text{O}_7$: an x-ray resonant scattering study," *J. Phys. Condens. Matter* **24**, 312202 (2012).
- [16] S. Boseggia, R. Springell, H. C. Walker, A. T. Boothroyd, D. Prabhakaran, D. Wernmeille, L. Bouchenoire, S. P. Collins, and D. F. McMorrow, "Antiferromagnetic order and domains in $\text{Sr}_3\text{Ir}_2\text{O}_7$ probed by x-ray resonant scattering," *Phys. Rev. B* **85**, 184432 (2012).
- [17] S. Boseggia, R. Springell, H. C. Walker, H. M. Rønnow, Ch. Rüegg, H. Okabe, M. Isobe, R. S. Perry, S. P. Collins, and D. F. McMorrow, "Robustness of Basal-Plane Antiferromagnetic Order and the $J_{\text{eff}}=1/2$ State in Single-Layer Iridate Spin-Orbit Mott Insulators," *Phys. Rev. Lett.* **110**, 117207 (2013).
- [18] M. Moretti Sala, M. Rossi, S. Boseggia, J. Akimitsu, N. B. Brookes, M. Isobe, M. Minola, H. Okabe, H. M. Rønnow, L. Simonelli, D. F. McMorrow, and G. Monaco, "Orbital occupancies and the putative $j_{\text{eff}} = \frac{1}{2}$ ground state in Ba_2IrO_4 : A combined oxygen K -edge XAS and RIXS study," *Phys. Rev. B* **89**, 121101(R) (2014).
- [19] Jung-ho Kim, D. Casa, M. H. Upton, T. Gog, Young-June Kim, J. F. Mitchell, M. van Veenendaal, M. Daghofer, J. van den Brink, G. Khaliullin, and B. J. Kim, "Magnetic Excitation Spectra of Sr_2IrO_4 Probed by Resonant Inelastic X-Ray Scattering: Establishing Links to Cuprate Superconductors," *Phys. Rev. Lett.* **108**, 177003 (2012).
- [20] Y. K. Kim, O. Krupin, J. D. Denlinger, A. Bostwick, E. Rotenberg, Q. Zhao, J. F. Mitchell, J. W. Allen, and B. J. Kim, "Fermi arcs in a doped pseudospin-1/2 Heisenberg antiferromagnet," *Science* **345**, 187–190 (2014).
- [21] Y. K. Kim, N. H. Sung, J. D. Denlinger, and B. J. Kim, "Observation of a d-wave gap in electron-doped Sr_2IrO_4 ," *Nat. Phys.* **12**, 37 (2015).
- [22] A. de la Torre, S. McKeown Walker, F. Y. Bruno, S. Riccò, Z. Wang, I. Gutierrez Lezama, G. Scheerer, G. Giriat, D. Jaccard, C. Berthod, T. K. Kim, M. Hoesch, E. C. Hunter, R. S. Perry, A. Tamai, and F. Baumberger, "Collapse of the Mott Gap and Emergence of a Nodal Liquid in Lightly Doped Sr_2IrO_4 ," *Phys. Rev. Lett.* **115**, 176402 (2015).
- [23] Y. J. Yan, M. Q. Ren, H. C. Xu, B. P. Xie, R. Tao, H. Y. Choi, N. Lee, Y. J. Choi, T. Zhang, and D. L. Feng, "Electron-Doped Sr_2IrO_4 : An Analogue of Hole-Doped Cuprate Superconductors Demonstrated by Scanning Tunneling Microscopy," *Phys. Rev. X* **5**, 041018 (2015).
- [24] H. Gretarsson, N. H. Sung, M. Höppner, B. J. Kim, B. Keimer, and M. Le Tacon, "Two-Magnon Raman Scattering and Pseudospin-Lattice Interactions in Sr_2IrO_4 and $\text{Sr}_3\text{Ir}_2\text{O}_7$," *Phys. Rev. Lett.* **116**, 136401 (2016).
- [25] X. Liu, M. P. M. Dean, Z. Y. Meng, M. H. Upton, T. Qi, T. Gog, Y. Cao, J. Q. Lin, D. Meyers, H. Ding, G. Cao, and J. P. Hill, "Anisotropic softening of magnetic excitations in lightly electron-doped Sr_2IrO_4 ," *Phys. Rev. B* **93**, 241102(R) (2016).
- [26] Jaehong Jeong, Yvan Sidis, Alex Louat, Vronique Brouet, and Philippe Bourges, "Time-reversal symmetry breaking hidden order in $\text{Sr}_2(\text{Ir,Rh})\text{O}_4$," *Nat. Commun.* **8**, 15119 (2017).
- [27] D. Pincini, J. G. Vale, C. Donnerer, A. de la Torre, E. C. Hunter, R. Perry, M. Moretti Sala, F. Baumberger, and D. F. McMorrow, "Anisotropic exchange and spin-wave damping in pure and electron-doped Sr_2IrO_4 ," *Phys. Rev. B* **96**, 075162 (2017).
- [28] Fa Wang and T. Senthil, "Twisted Hubbard Model for Sr_2IrO_4 : Magnetism and Possible High Temperature Superconductivity," *Phys. Rev. Lett.* **106**, 136402 (2011).
- [29] Hiroshi Watanabe, Tomonori Shirakawa, and Seiji Yunoki, "Monte Carlo Study of an Unconventional Superconducting Phase in Iridium Oxide $J_{\text{eff}}=1/2$ Mott Insulators Induced by Carrier Doping," *Phys. Rev. Lett.* **110**, 027002 (2013).
- [30] Yang Yang, Wan-Sheng Wang, Jin-Guo Liu, Hua Chen, Jian-Hui Dai, and Qiang-Hua Wang, "Superconductivity in doped Sr_2IrO_4 : A functional renormalization group study," *Phys. Rev. B* **89**, 094518 (2014).
- [31] Zi Yang Meng, Yong Baek Kim, and Hae-Young Kee, "Odd-Parity Triplet Superconducting Phase in Multi-orbital Materials with a Strong Spin-Orbit Coupling: Application to Doped Sr_2IrO_4 ," *Phys. Rev. Lett.* **113**, 177003 (2014).
- [32] Sae Hwan Chun, Jong-Woo Kim, Jung-ho Kim, H. Zheng, Constantinos C. Stoumpos, C. D. Malliakas, J. F. Mitchell, Kavita Mehlawat, Yogesh Singh, Y. Choi, T. Gog, A. Al-Zein, M. Moretti Sala, M. Krisch, J. Chaloupka, G. Jackeli, G. Khaliullin, and B. J. Kim, "Direct evidence for dominant bond-directional interactions in a honeycomb lattice iridate Na_2IrO_3 ," *Nat. Phys.* **11**, 462 (2015).
- [33] M. Hermanns, I. Kimchi, and J. Knolle, "Physics of the Kitaev Model: Fractionalization, Dynamic Correlations, and Material Connections," *Annu. Rev. Condens. Matter Phys.* **9**, 17–33 (2018).
- [34] Yogesh Singh and P. Gegenwart, "Antiferromagnetic Mott insulating state in single crystals of the honeycomb lattice material Na_2IrO_3 ," *Phys. Rev. B* **82**, 064412 (2010).
- [35] Yogesh Singh, S. Manni, J. Reuther, T. Berlijn, R. Thomale, W. Ku, S. Trebst, and P. Gegenwart, "Relevance of the Heisenberg-Kitaev Model for the Honeycomb Lattice Iridates $A_2\text{IrO}_3$," *Phys. Rev. Lett.* **108**, 127203 (2012).
- [36] Kavita Mehlawat, A. Thamizhavel, and Yogesh Singh, "Heat capacity evidence for proximity to the Kitaev quantum spin liquid in $A_2\text{IrO}_3$ ($A = \text{Na}, \text{Li}$)," *Phys. Rev. B* **95**, 144406 (2017).
- [37] T. Takayama, A. Kato, R. Dinnebier, J. Nuss, H. Kono, L. S. I. Veiga, G. Fabbri, D. Haskel, and H. Takagi, "Hyperhoneycomb Iridate $\beta\text{-Li}_2\text{IrO}_3$ as a Platform for Kitaev Magnetism," *Phys. Rev. Lett.* **114**, 077202 (2015).
- [38] K. A. Modic, Tess E. Smidt, Itamar Kimchi, Nicholas P. Breznay, Alun Biffin, Sungkyun Choi, Roger D. Johnson, Radu Coldea, Pilanda Watkins-Curry, Gregory T.

- McCandless, Julia Y. Chan, Felipe Gandara, Z. Islam, Ashvin Vishwanath, Arkady Shekhter, Ross D. McDonald, and James G. Analytis, “Realization of a three-dimensional spin-anisotropic harmonic honeycomb iridate,” *Nat. Commun.* **5**, 4203 (2014).
- [39] Alexei Kitaev, “Anyons in an exactly solved model and beyond,” *Ann. Phys.* **321**, 2 – 111 (2006).
- [40] Jiří Chaloupka, George Jackeli, and Giniyat Khaliullin, “Kitaev-Heisenberg Model on a Honeycomb Lattice: Possible Exotic Phases in Iridium Oxides $A_2\text{IrO}_3$,” *Phys. Rev. Lett.* **105**, 027204 (2010).
- [41] S. K. Choi, R. Coldea, A. N. Kolmogorov, T. Lancaster, I. I. Mazin, S. J. Blundell, P. G. Radaelli, Yogesh Singh, P. Gegenwart, K. R. Choi, S.-W. Cheong, P. J. Baker, C. Stock, and J. Taylor, “Spin Waves and Revised Crystal Structure of Honeycomb Iridate Na_2IrO_3 ,” *Phys. Rev. Lett.* **108**, 127204 (2012).
- [42] Jiří Chaloupka, George Jackeli, and Giniyat Khaliullin, “Zigzag Magnetic Order in the Iridium Oxide Na_2IrO_3 ,” *Phys. Rev. Lett.* **110**, 097204 (2013).
- [43] A. Banerjee, C. A. Bridges, J.-Q. Yan, A. A. Aczel, L. Li, M. B. Stone, G. E. Granroth, M. D. Lumsden, Y. Yiu, J. Knolle, S. Bhattacharjee, D. L. Kovrizhin, R. Moessner, D. A. Tennant, D. G. Mandrus, and S. E. Nagler, “Proximate Kitaev quantum spin liquid behaviour in a honeycomb magnet,” *Nat. Mater.* **15**, 733 (2016).
- [44] Stephen M. Winter, Ying Li, Harald O. Jeschke, and Roser Valentí, “Challenges in design of Kitaev materials: Magnetic interactions from competing energy scales,” *Phys. Rev. B* **93**, 214431 (2016).
- [45] Yoshihiro Doi and Yukio Hinatsu, “The structural and magnetic characterization of 6H-perovskite-type oxides $\text{Ba}_3\text{LnIr}_2\text{O}_9$ (Ln = Y, lanthanides),” *J. Phys. Condens. Matter* **16**, 2849–2860 (2004).
- [46] Takeshi Sakamoto, Yoshihiro Doi, and Yukio Hinatsu, “Crystal structures and magnetic properties of 6H-perovskite-type oxides $\text{Ba}_3\text{M}\text{Ir}_2\text{O}_9$ (M = Mg, Ca, Sc, Ti, Zn, Sr, Zr, Cd and In),” *J. Solid State Chem.* **179**, 2595 – 2601 (2006).
- [47] A. Revelli, M. Moretti Sala, G. Monaco, P. Becker, L. Bohatý, M. Hermanns, T. C. Koethe, T. Fröhlich, P. Warzanowski, T. Lorenz, S. V. Streltsov, P. H. M. van Loosdrecht, D. I. Khomskii, J. van den Brink, and M. Grüninger, “Resonant inelastic x-ray incarnation of Young’s double-slit experiment,” *Sci. Adv.* **5** (2019), 10.1126/sciadv.aav4020.
- [48] Kenya Ohgushi, Jun-ichi Yamaura, Hiroyuki Ohsumi, Kunihisa Sugimoto, Soshi Takeshita, Akihisa Tokuda, Hidenori Takagi, Masaki Takata, and Taka-hisa Arima, “Resonant X-ray Diffraction Study of the Strongly Spin-Orbit-Coupled Mott Insulator CaIrO_3 ,” *Phys. Rev. Lett.* **110**, 217212 (2013).
- [49] Nikolay A. Bogdanov, Vamshi M. Katukuri, Hermann Stoll, Jeroen van den Brink, and Liviu Hozoi, “Post-perovskite CaIrO_3 : A $j = 1/2$ quasi-one-dimensional antiferromagnet,” *Phys. Rev. B* **85**, 235147 (2012).
- [50] K. Ohgushi, H. Gotou, T. Yagi, Y. Kiuchi, F. Sakai, and Y. Ueda, “Metal-insulator transition in $\text{Ca}_{1-x}\text{Na}_x\text{IrO}_3$ with post-perovskite structure,” *Phys. Rev. B* **74**, 241104(R) (2006).
- [51] J.-G. Cheng, J.-S. Zhou, J. B. Goodenough, Y. Sui, Y. Ren, and M. R. Suchomel, “High-pressure synthesis and physical properties of perovskite and post-perovskite $\text{Ca}_{1-x}\text{Sr}_x\text{IrO}_3$,” *Phys. Rev. B* **83**, 064401 (2011).
- [52] J. Gunasekera, Y. Chen, J. W. Kremenak, P. F. Miceli, and D. K. Singh, “Mott insulator-to-metal transition in yttrium-doped CaIrO_3 ,” *J. Physics Condens. Matter* **27**, 052201 (2015).
- [53] J. Gunasekera, L. Harriger, A. Dahal, T. Heitmann, G. Vignale, and D. K. Singh, “Magnetic fluctuations driven insulator-to-metal transition in $\text{CaIr}_{1-x}\text{Ru}_x\text{O}_3$,” *Sci. Rep.* **5**, 18047 (2015).
- [54] M Moretti Sala, C. Henriquet, L. Simonelli, R. Verbeni, and G. Monaco, “High energy-resolution set-up for Ir L_3 edge RIXS experiments,” *J. Electron Spectros. Relat. Phenomena* **188**, 150–154 (2013).
- [55] M. Moretti Sala, K. Martel, C. Henriquet, A. Al Zein, L. Simonelli, Ch. J. Sahle, H. Gonzalez, M.-C. Lagier, C. Ponchut, S. Huotari, R. Verbeni, M. Krisch, and G. Monaco, “A high-energy-resolution resonant inelastic X-ray scattering spectrometer at ID20 of the European Synchrotron Radiation Facility,” *J. Synchrotron Rad.* **25**, 580–591 (2018).
- [56] C Ponchut, J M Rigal, J Clément, E Papillon, A Homs, and S Petitdemange, “MAXIPIX, a fast readout photon-counting X-ray area detector for synchrotron applications,” *J. Instrum.* **6**, C01069–C01069 (2011).
- [57] Peter J. E. M. van der Linden, Marco Moretti Sala, Christian Henriquet, Matteo Rossi, Kenya Ohgushi, Francois Fauth, Laura Simonelli, Carlo Marini, Edmundo Fraga, Claire Murray, Jonathan Potter, and Michael Krisch, “A compact and versatile dynamic flow cryostat for photon science,” *Rev. Sci. Instrum.* **87**, 115103 (2016).
- [58] M. Moretti Sala, K. Ohgushi, A. Al-Zein, Y. Hirata, G. Monaco, and M. Krisch, “ CaIrO_3 : A Spin-Orbit Mott Insulator Beyond the $j_{\text{eff}} = 1/2$ Ground State,” *Phys. Rev. Lett.* **112**, 176402 (2014).
- [59] Sun-Woo Kim, Chen Liu, Hyun-Jung Kim, Jun-Ho Lee, Yongxin Yao, Kai-Ming Ho, and Jun-Hyung Cho, “Nature of the Insulating Ground State of the $5d$ Postperovskite CaIrO_3 ,” *Phys. Rev. Lett.* **115**, 096401 (2015).
- [60] Vijeta Singh and J. J. Pulikkotil, “Post-perovskite CaIrO_3 : a conventional Slater type antiferromagnetic insulator,” *Phys. Chem. Chem. Phys.* **18**, 26300–26305 (2016).
- [61] Luuk J. P. Ament, Giniyat Khaliullin, and Jeroen van den Brink, “Theory of resonant inelastic x-ray scattering in iridium oxide compounds: Probing spin-orbit-entangled ground states and excitations,” *Phys. Rev. B* **84**, 020403(R) (2011).
- [62] M. Moretti Sala, S. Boseggia, D. F. McMorrow, and G. Monaco, “Resonant X-Ray Scattering and the $j_{\text{eff}}=1/2$ Electronic Ground State in Iridate Perovskites,” *Phys. Rev. Lett.* **112**, 026403 (2014).
- [63] M. Moretti Sala, M. Rossi, A. Al-Zein, S. Boseggia, E. C. Hunter, R. S. Perry, D. Prabhakaran, A. T. Boothroyd, N. B. Brookes, D. F. McMorrow, G. Monaco, and M. Krisch, “Crystal field splitting in $\text{Sr}_{n+1}\text{Ir}_n\text{O}_{3n+1}$ ($n = 1, 2$) iridates probed by x-ray Raman spectroscopy,” *Phys. Rev. B* **90**, 085126 (2014).
- [64] M. Moretti Sala, V. Schnell, S. Boseggia, L. Simonelli, A. Al-Zein, J. G. Vale, L. Paolasini, E. C. Hunter, R. S. Perry, D. Prabhakaran, A. T. Boothroyd, M. Krisch, G. Monaco, H. M. Rønnow, D. F. McMorrow, and F. Mila, “Evidence of quantum dimer excitations in $\text{sr}_3\text{ir}_2\text{o}_7$,” *Phys. Rev. B* **92**, 024405 (2015).
- [65] T. Giamarchi, *Quantum Physics in One Dimension*, International Series of Monographs on Physics (Clarendon

- Press, 2004).
- [66] Michael Karbach, Gerhard Müller, A. Hamid Bougourzi, Andreas Fledderjohann, and Karl-Heinz Mütter, “Two-spinon dynamic structure factor of the one-dimensional $s=1/2$ Heisenberg antiferromagnet,” *Phys. Rev. B* **55**, 12510–12517 (1997).
- [67] I. A. Zaliznyak, H. Woo, T. G. Perring, C. L. Broholm, C. D. Frost, and H. Takagi, “Spinons in the Strongly Correlated Copper Oxide Chains in SrCuO_2 ,” *Phys. Rev. Lett.* **93**, 087202 (2004).
- [68] Bella Lake, D. Alan Tennant, Chris D. Frost, and Stephen E. Nagler, “Quantum criticality and universal scaling of a quantum antiferromagnet,” *Nat. Mater.* **4**, 329 (2005).
- [69] Jean-Sébastien Caux and Rob Hagemans, “The four-spinon dynamical structure factor of the Heisenberg chain,” *J. Stat. Mech.: Theory Exp.* **2006**, P12013–P12013 (2006).
- [70] Bella Lake, Alexei M. Tsvelik, Susanne Notbohm, D. Alan Tennant, Toby G. Perring, Manfred Reehuis, Chinnathambi Sekar, Gernot Krabbes, and Bernd Büchner, “Confinement of fractional quantum number particles in a condensed-matter system,” *Nat. Phys.* **6**, 50 (2009).
- [71] J. Schlappa, K. Wohlfeld, K. J. Zhou, M. Mourigal, M. W. Haverkort, V. N. Strocov, L. Hozoi, C. Monney, S. Nishimoto, S. Singh, A. Revcolevschi, J.-S. Caux, L. Patthey, H. M. Rønnow, J. van den Brink, and T. Schmitt, “Spinorbital separation in the quasi-one-dimensional Mott insulator Sr_2CuO_3 ,” *Nature* **485**, 82 (2012).
- [72] Martin Mourigal, Mechthild Enderle, Axel Klöpperpieper, Jean-Sébastien Caux, Anne Stunault, and Henrik M. Rønnow, “Fractional spinon excitations in the quantum Heisenberg antiferromagnetic chain,” *Nat. Phys.* **9**, 435 (2013).
- [73] L. S. Wu, W. J. Gannon, I. A. Zaliznyak, A. M. Tsvelik, M. Brockmann, J.-S. Caux, M. S. Kim, Y. Qiu, J. R. D. Copley, G. Ehlers, A. Podlesnyak, and M. C. Aronson, “Orbital-exchange and fractional quantum number excitations in an f-electron metal, $\text{Yb}_2\text{Pt}_2\text{Pb}$,” *Science* **352**, 1206–1210 (2016).
- [74] A. K. Bera, B. Lake, F. H. L. Essler, L. Vanderstraeten, C. Hubig, U. Schollwöck, A. T. M. N. Islam, A. Schneidewind, and D. L. Quintero-Castro, “Spinon confinement in a quasi-one-dimensional anisotropic Heisenberg magnet,” *Phys. Rev. B* **96**, 054423 (2017).
- [75] R. Fumagalli, J. Hoyerhagen, D. Betto, R. Arpaia, M. Rossi, D. Di Castro, N. B. Brookes, M. Moretti Sala, M. Daghofer, L. Braicovich, K. Wohlfeld, and G. Ghiringhelli, “Mobile orbitons in Ca_2CuO_3 : Crucial role of Hund’s exchange,” *Phys. Rev. B* **101**, 205117 (2020).
- [76] Gerhard Müller, Harry Thomas, Hans Beck, and Jill C. Bonner, “Quantum spin dynamics of the antiferromagnetic linear chain in zero and nonzero magnetic field,” *Phys. Rev. B* **24**, 1429–1467 (1981).
- [77] Marc Bocquet, Fabian H. L. Essler, Alexei M. Tsvelik, and Alexander O. Gogolin, “Finite-temperature dynamical magnetic susceptibility of quasi-one-dimensional frustrated spin- $\frac{1}{2}$ Heisenberg antiferromagnets,” *Phys. Rev. B* **64**, 094425 (2001).
- [78] D. J. Scalapino, Y. Imry, and P. Pincus, “Generalized Ginzburg-Landau theory of pseudo-one-dimensional systems,” *Phys. Rev. B* **11**, 2042–2048 (1975).
- [79] H. J. Schulz, “Dynamics of Coupled Quantum Spin Chains,” *Phys. Rev. Lett.* **77**, 2790–2793 (1996).
- [80] A. Zheludev, S. Raymond, L.-P. Regnault, F. H. L. Essler, K. Kakurai, T. Masuda, and K. Uchinokura, “Polarization dependence of spin excitations in $\text{BaCu}_2\text{Si}_2\text{O}_7$,” *Phys. Rev. B* **67**, 134406 (2003).
- [81] M. Enderle, B. Fåk, H.-J. Mikeska, R. K. Kremer, A. Prokofiev, and W. Assmus, “Two-Spinon and Four-Spinon Continuum in a Frustrated Ferromagnetic Spin- $1/2$ Chain,” *Phys. Rev. Lett.* **104**, 237207 (2010).
- [82] J. C. Leiner, Joosung Oh, A. I. Kolesnikov, M. B. Stone, Manh Duc Le, E. P. Kenny, B. J. Powell, M. Mourigal, E. E. Gordon, M.-H. Whangbo, J.-W. Kim, S.-W. Cheong, and Je-Geun Park, “Magnetic excitations of the Cu^{2+} quantum spin chain in $\text{Sr}_3\text{CuPtO}_6$,” *Phys. Rev. B* **97**, 104426 (2018).
- [83] Tôru Moriya, “Anisotropic Superexchange Interaction and Weak Ferromagnetism,” *Phys. Rev.* **120**, 91–98 (1960).